British Journal of Pharmacology

DOI:10.1111/j.1476-5381.2010.01078.x
www.brjpharmacol.org

RESEARCH PAPER

Impaired neoangiogenesis in β_2–adrenoceptor gene-deficient mice: restoration by intravascular human β_2–adrenoceptor gene transfer and role of NFκB and CREB transcription factors

Michele Ciccarelli[1,2]*, Daniela Sorriento[1]*, Ersilia Cipolletta[1], Gaetano Santulli[1], Anna Fusco[1], Rui-Hai Zhou[2], Andrea D. Eckhart[2], Karsten Peppel[2], Walter J. Koch[2], Bruno Trimarco[1] and Guido Iaccarino[1]

[1]*Dipartimento di Medicina Clinica, Scienze Cardiovascolari ed Immunologiche, Università Federico II, Napoli, Italy, and* [2]*Center for Translational Medicine, Thomas Jefferson University, Philadelphia, PA, USA*

Correspondence
Guido Iaccarino, Medicina Clinica, Scienze Cardiovascolari ed Immunologiche, Federico II University, Via Pansini 5; Edificio 2, 80131 Naples, Italy. E-mail: guiaccar@unina.it

*These Authors contributed equally to this paper.

Keywords
adrenergic signalling; gene therapy; ischaemic hindlimb; NFκB activity

Received
7 May 2010
Revised
22 September 2010
Accepted
25 September 2010

BACKGROUND AND PURPOSE

There is much evidence supporting the role of β_2-adrenoceptors (β_2AR) in angiogenesis but the mechanisms underlying their effects have not been elucidated. Hence, we studied post-ischaemic angiogenesis in the hindlimb (HL) of β_2AR knock-out mice (β_2AR–/–) *in vivo* and explored possible molecular mechanisms *in vitro*.

EXPERIMENTAL APPROACH

Femoral artery resection (FAR) was performed in wild-type and β_2AR–/– mice and adaptive responses to chronic HL ischaemia were explored; blood flow was measured by ultrasound and perfusion of dyed beads, bone rarefaction, muscle fibrosis and skin thickness were evaluated by immunoflourescence and morphometric analysis. Intrafemoral delivery of an adenovirus encoding the human β_2AR (ADβ_2AR) was used to reinstate β_2ARs in β_2AR–/– mice. Molecular mechanisms were investigated in mouse-derived aortic endothelial cells (EC) *in vitro*, focusing on NFκB activation and transcriptional activity.

RESULTS

Angiogenesis was severely impaired in β_2AR–/– mice subjected to FAR, but was restored by gene therapy with ADβ_2AR. The proangiogenic responses to a variety of stimuli were impaired in β_2AR–/– EC *in vitro*. Moreover, removal of β_2ARs impaired the activation of NFκB, a transcription factor that promotes angiogenesis; neither isoprenaline (stimulates βARs) nor TNFα induced NFκB activation in β_2AR$^{-/-}$ EC. Interestingly, cAMP response element binding protein (CREB), a transcription factor that counter regulates NFκB, was constitutively increased in β_2AR$^{-/-}$ ECs. ADβ_2AR administration restored β_2AR membrane density, reduced CREB activity and reinstated the NFκB response to isoprenaline and TNFα.

CONCLUSIONS AND IMPLICATIONS

Our results suggest that β_2ARs control angiogenesis through the tight regulation of nuclear transcriptional activity.

Abbreviations

ADβ_2AR, gene therapy with adenovirus encoding the human β_2AR; ADU, arbitrary densitometry units; β_2AR, β_2 adrenoceptor; β_2AR–/–, β_2AR knock-out mice; BF, blood flow; CREB, cAMP response element binding protein; EC, endothelial cell; US, ultrasound; VEGF, vascular endothelial growth factor

Introduction

Little is known about the role of the β_2-adrenoceptor (β_2AR) in the vasculature. Recently, our group and others have begun to elucidate the mechanisms of β_2AR control of vascular functions (Lembo *et al.*, 1997; Ferro *et al.*, 1999) and showed that this receptor can activate eNOS in an Akt-dependent manner and induce release of nitric oxide (NO) at the endothelium (Iaccarino *et al.*, 2002; 2004). We have also shown that the adenoviral-mediated endothelial overexpression of the β_2AR regulates post-ischaemic angiogenesis (Iaccarino *et al.*, 2005), to the extent that β_2ARs can correct impaired angiogenesis in animal models of cardiovascular disease such as the spontaneously hypertensive rat (Iaccarino *et al.*, 2002; 2005). The mechanisms underlying β_2AR-regulated angiogenesis have still not been elucidated. One possible explanation is that receptors such as the β_2AR are able to regulate the transcriptional activity of the cell, in order to promote the release of proangiogenic cytokines such as vascular endothelial growth factor (VEGF). Indeed, β_2AR overexpression results in VEGF accumulation in the culture medium of endothelial cells. VEGF has a transcriptional regulation that is controlled by the hypoxia responsive transcription factor-1 (HIF-1), and also by NFκB, which is known to be activated downstream by tumour necrosis factor receptors (TNF-R) superfamily-members and some G protein-coupled, seven transmembrane (7TM) receptors (GPCRs) (Ye, 2001).

The role of NFκB in angiogenesis is well established, and is linked to its ability to regulate inflammatory cytokine production in many cellular types; these include the endothelium, infiltrating macrophages, vascular smooth muscle cells and pericytes, and skeletal muscle cells. In this context, receptor and transcription factors are major players, allowing the finely tuned response of different cell types. Therefore, NFκB represents a particularly apt subject for our investigation on the signal transduction mechanisms underlying the proangiogenic effects of β_2ARs.

The β_2AR knock-out (β_2AR–/–) mouse model has already proved useful to unveil specific molecular features of the β_2AR (Chruscinski *et al.*, 1999; Shenoy *et al.*, 2006). We therefore exploited such a model to investigate the adaptive responses to chronic hindlimb (HL) ischaemia in a β_2AR-negative (β_2AR–/–) situation. Furthermore, using adenoviral-mediated gene transfer, we reconstituted membrane β_2AR expression in the ischaemic HL. *In vitro*, we explored the possible mechanisms accounting for β_2AR's beneficial effects on angiogenesis, focusing particularly on NFκB activation and transcriptional activity.

Methods

Mouse strain and surgical procedures

Previously described β_2AR–/– and β_2AR+/+ mice (age 14–18 weeks) were used in this study (Chruscinski *et al.*, 1999). Founders were provided by courtesy of Brian Kobilka, Stanford University, CA. Mice were bred in heterozygousity and homozygous β_2AR–/– or β_2AR+/+ male littermates were used as the study and control population. All procedures were approved by the Thomas Jefferson University Institutional Animal Care and Use Committee and the Federico II University Ethical Committee for Animal Research. Mice were anaesthetized with a mixture of ketamine (100 mg·kg^{-1}) and xylazine (3 mg·kg^{-1}) and the right common femoral artery was isolated and removed. In a group of β_2AR–/– mice (n = 20), we placed a silastic catheter into the femoral artery distal to the resection, through which a solution containing 10^{11} tvp of either an adenovirus encoding for LacZ or the human β_2AR gene was infused into the HL and allowed to remain there for 30 min while the saphenous vein was temporarily occluded (Santulli *et al.*, 2009a). Afterwards, the virus was removed through the catheter, the common femoral artery removed and the wound closed in layers. With this manoeuvre, we ascertained that endothelial cells, vascular smooth muscle cells and skeletal myocytes of the hindlimb express the transgene carried by the viral vector, as found previously (Santulli *et al.*, 2009a). Mice were checked daily for fur loss, skin lesions (blistering), necrosis, self-inflicted amputations of the ischaemic hindlimb. Surgical aftercare and distress surveillance were performed according to institution's guidelines.

Blood flow determination

Blood flow (BF) in the posterior tibial artery of ischaemic and non-ischaemic HL was evaluated by ultrasound (US) (using a VisualSONICS VeVo 770 imaging system with a 710 MHz scanhead) in isofluorane-anaesthetized mice (2% v·v^{-1}) immediately after surgery and at days 3, 7, 10 and 14 thereafter. We measured maximal velocity (Vmax) and maximal diameter of the vessel. After calculation of the vessel area, BF was calculated using the formula: BF = Vmax/vessel area (Santulli *et al.*, 2009a). Data are expressed as ischaemic to non-ischaemic ratio. Fourteen days after surgery, mice were anaesthetized as above, and a PE 10 catheter was placed into the abdominal aorta through the left common carotid, as previously described (Iaccarino *et al.*, 2002). Maximal vasodilatation was obtained by administration of nitroglycerin (2 μg i.a.) followed by injection of 3×10^6 orange-dyed beads (15 μm diameter, Triton Technologies, San Diego, CA, USA). Animals were then killed by cervical dislocation, samples of the gastrocnemius muscle from the ischaemic and non-ischaemic HL were collected and frozen with liquid nitrogen and stored at –80°C. Next, the samples were homogenized and digested according to manufacturer protocol; the beads were collected and suspended in DMTF. The release of dye was assessed by light absorption at 450 nm (Santulli *et al.*, 2009a). Data are expressed as ischaemic to non-ischaemic muscle ratio.

Immunofluorescence and morphology

At 14 days, we used B mode US for morphological analysis of the ischaemic and controlateral hindlimbs. In particular, we evaluated bone rarefaction, muscle fibrosis and skin thickness, all processes that are associated with HL ischaemia (Santulli *et al.*, 2009b).

The anterior tibial muscle was isolated and harvested for immunostaining as described previously (Zhou *et al.*, 2003). Specimens were fixed in 4% paraformaldehyde and then embedded in paraffin. A series of cross-sections (6 μm) were obtained. Rat anti-CD31 antibody (1:50, BD Pharmingen, CA) and rabbit anti-von Willebrand (vW) factor (1:50, DAKO,

Carpinteria, CA) were used as primary antibodies for double staining of endothelial cells. As a negative control, normal rat and rabbit IgG were used instead of the primary antibody. The primary antibodies were recognized by Alexa Fluor 594 goat anti-rat (Green) and Alexa Fluor 488 goat anti-rabbit (Blue) secondary antibodies (1:100), respectively (Molecular Probes, Eugene, Oregan). Nuclei were counterstained with VECTASHIELD mounting medium with DAPI (Red) (Vector, Burlingame, CA). Immunofluorescence was visualized under a fluorescence microscope (Olympus IX71, Olympus, Center Valley, CA, USA) and the number of capillaries per 20 fields was measured on each section by two independent operators (M.C., R.H.Z.), blinded to treatment. Another series of tissue sections were stained with haematoxylin/eosin (H&E) for morphological analysis.

βAR radioligand binding

Membrane fractions were obtained from quadricep muscle homogenates by centrifugation as previously described (Iaccarino *et al.*, 1998). Total receptor density was assessed by βAR radioligand binding studies using the non-selective βAR antagonist [^{125}I]-cyanopindolol (^{125}I-CYP), as described previously (Iaccarino *et al.*, 2001b). The percentage of β_2ARs was calculated from the high affinity binding subpopulation using GraphPad Prism.

Adenoviral constructs

We used adenoviral vectors encoding for the human wild-type β_2AR gene (Adβ_2AR) and the LacZ (control virus) as previously described (Iaccarino *et al.*, 2002; 2005; Ciccarelli *et al.*, 2007).

Cell culture

Aortic endothelial cells (ECs) from β_2AR–/– and β_2AR+/+ mice were isolated as previously described (Iaccarino *et al.*, 2002). Vessels were cut into rings, placed on matrigel, incubated in DMEM supplemented with 20% FBS and EC growth supplement (10 mg · 100 mL^{-1}), and incubated at 37°C in 5% CO_2. After 7 days, aortic rings were removed, and the ECs remaining on matrigel were expanded in DMEM containing 10% FBS.

Western blotting

Cells were deprived of serum overnight, exposed to agonists and lysed in RIPA/SDS buffer (50 mmol·L^{-1} Tris-HCl, pH 7.5, 150 mmol·L^{-1} NaCl, 1% NP-40, 0.25% deoxycholate, 9.4 mg·50 mL^{-1} sodium orthovanadate, 20% SDS). Protein concentration was determined using a BSA assay kit (Pierce, Thermoscientific, Rockford, IL, USA). IκBα was immunoprecipitated from total lysates with anti-IκBα antibody and protein A/G agarose. Immunocomplexes or total lysates were electrophoresed by SDS/PAGE and transferred to a nitrocellulose filter. Total IκBα and β_2AR were visualized by specific antibodies (Santacruz, Santa Cruz, CA, USA), anti-rabbit horseradish peroxidase–conjugated secondary antibody (Santacruz) and standard chemiluminescence (Pierce). Autoradiographies were then digitalized and densitometry quantification performed using dedicated software (ImageQuant, GE HealthCare, Milano, Italy). Data are presented as arbitrary densitometry units (ADU) after normalization for actin. In other experiments, cells were infected with Adβ_2AR at a rate of 20:1.

VEGF quantification

Aortic ECs from β_2AR–/– and β_2AR+/+ mice were deprived of serum overnight and then stimulated with isoprenaline (Iso) for 6 h. Culture medium was collected and VEGF was immunoprecipitated with anti-VEGF antibody (Santacruz) and protein A/G agarose (Santacruz). After being extensively washed, the immunocomplexes were electrophoresed by SDS/PAGE and transferred to nitrocellulose; VEGF was visualized by specific antibody (Santacruz), anti-rabbit HRP-conjugated secondary antibody (Santacruz) and standard chemiluminescence (Pierce). For our analysis, we examined the Western blot band corresponding to VEGF 164 isoform.

Cell transfection and luciferase assay

Transient transfection was performed using Lipofectamine 2000 (Invitrogen, Paisley, UK) according to manufacturer's instruction. Aortic ECs from β_2AR–/– and β_2AR+/+ mice were transfected with plasmid expression vectors coding cAMP response element binding protein (CREB) and IκB plasmids (Sorriento *et al.*, 2009; 2010) used for signal transduction studies, or with a κB-luciferase reporter and β-galactosidase for NFκB activity. In this latter case, 24 h after transfection, cells were deprived of serum overnight and stimulated with TNFα (20 ng·mL^{-1}), as positive control, and Iso (10^{-7} mol·L^{-1}) for 1, 3 and 6 h. Lysates were analysed using the luciferase assay system with reporter lysis buffer from Promega and measured in a β-counter. Relative luciferase activity was normalized against the co-expressed β-galactosidase activity to overcome variations in transfection efficiency between samples. In other experiments, cells were stimulated with Iso (10^{-7} mol·L^{-1}) or TNFα (20 ng·mL^{-1}) for 3 h (Santulli *et al.*, 2009b).

Tube formation assay

When plated on matrigel (Becton Dickinson, Bedford, MA, USA), ECs organize themselves into a network-like structure, resembling sinusoids of immature vessels (Ciccarelli *et al.*, 2008). Six-well multidishes were coated with growth factor-reduced matrigel (10 mg·mL^{-1}) according to the manufacturer's instructions. Control and β_2AR–/– ECs (2 × 10^5) were incubated at 37°C for 12 h in 1 mL of DMEM medium. Tube formation was defined as a structure exhibiting a length four times its width. Network formation was observed using an inverted phase-contrast microscope (ZEISS). Representative fields were taken, and the average of the total number of complete tubes formed by cells was counted in 15 random fields by two independent investigators (D.S and E.C.).

RT PCR

Total RNA was isolated from ECs deprived of serum overnight or mouse hindlimb muscle using Trizol reagent (Invitrogen) and cDNA was synthesized by means of Thermo-Script RT-PCR System (Invitrogen), following the manufacturer's instruction. After reverse transcription, real-time quantitative polymerase chain reaction (RT-PCR) was performed with the SYBR Green Real Time PCR master mix kit (Applied Biosystems, Carlsbad, CA, USA). The reaction was visualized with

SYBR Green Analysis (Applied Biosystem) software on a StepOne thermocycler (Applied Biosystem). Primers for VEGF-165 and GAPDH gene analysis were as previously described (Sorriento *et al.*, 2009).

Statistical analysis

Data are presented as mean ± SEM. Each experiment was performed from three to five times. *P* values were calculated by Student's *t*-test or two-way ANOVA as appropriate. For distribution statistics, the chi-squared test was performed.

The nomenclature conforms to the British Journal of Pharmacology's 'Guide to Receptors and Channels' (Alexander *et al.*, 2009).

Results

In vivo *post-ischaemic angiogenesis*

Blood perfusion evaluation. As shown in Figure 1A, compared to β_2AR proficient controls, hindlimbs from β_2AR–/– mice present a significantly lower βAR membrane-density. Intra-

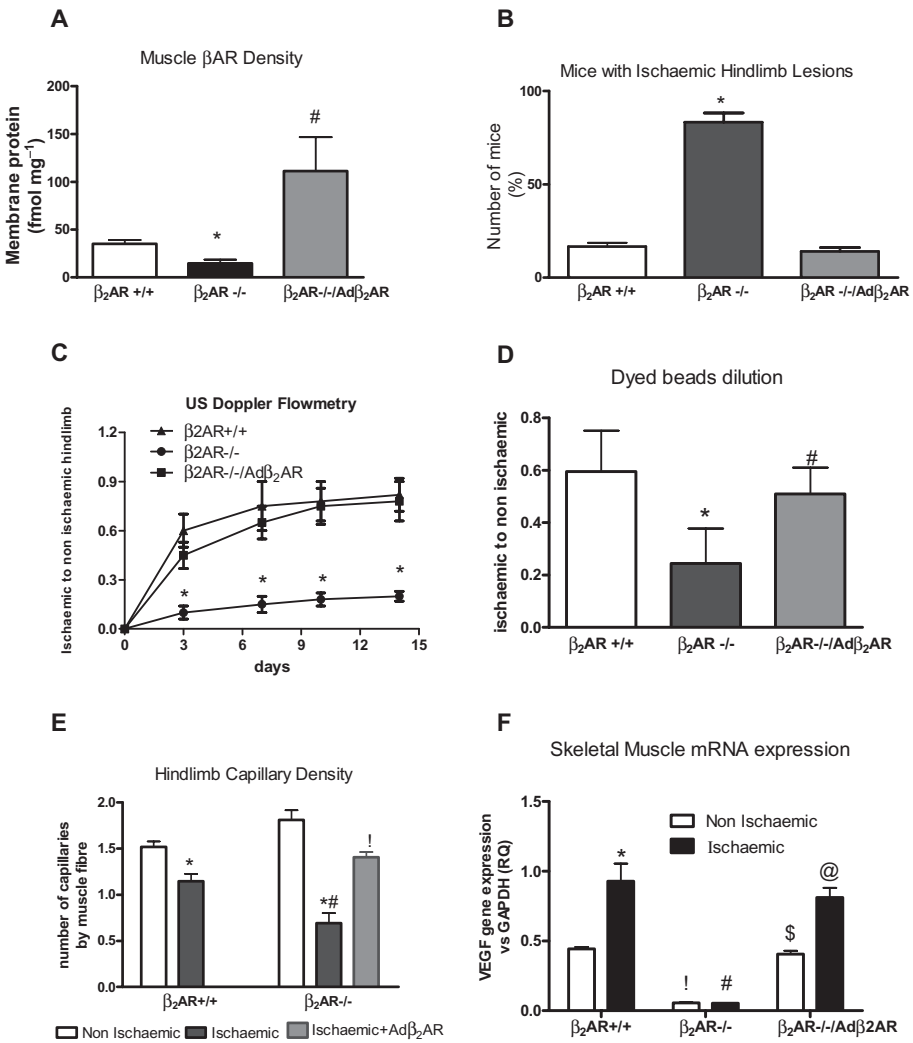

Figure 1

β_2AR knock-out exacerbated the symptoms of ischaemia and impaired perfusion and angiogenesis in ischaemic hindlimbs of mice. (A) Effects of adenoviral-mediated gene transfer on βAR levels (*$P < 0.05$ β_2AR–/– vs. β_2AR+/+; # $P < 0.05$, β_2AR–/–/ADβ_2AR vs. β_2AR–/–, $n = 3$ to 5). (B) Ischaemia-induced skin lesions in β_2AR–/– and β_2AR+/+ hindlimbs (HLs) (* $P < 0.05$ β_2AR–/– vs. β_2AR+/+, χ^2test, $n = 10$ per group). (C) HL blood flow over 14 days in β_2AR+/+, β_2AR–/–, and Adβ_2AR-treated β_2AR–/– ischaemic HL, as measured by US Doppler. ADβ_2AR ameliorated blood perfusion in the ischaemic HL (*$P < 0.05$ β_2AR–/– vs. β_2AR+/+; # $P < 0.05$, ADβ_2AR vs. β_2AR–/–; $n = 10$ per group). (D) Blood perfusion in the ischaemic HL as evaluated by dyed beads dilution method (*$P < 0.05$ β_2AR–/– vs. β_2AR+/+; # $P < 0.05$, β_2AR–/–/Adβ_2AR vs. β_2AR–/–; $n = 10$ per group). (E) HL muscle capillary density. (*$P < 0.05$ ischaemic vs. non-ischaemic muscle; #$P < 0.05$ β_2AR–/–vs. β_2AR+/+; ! $P < 0.05$, β_2AR–/–/Adβ_2AR vs. β_2AR–/–; $n = 5$ per each group). (F) VEGF gene expression in ischaemic gastrocnemius muscle 3 days after femoral artery ligation and resection (* $P < 0.05$ vs. non-ischaemic, $n = 3$; ! $P < 0.01$ vs. non-ischaemic β_2AR +/+; # $P < 0.01$ vs. ischaemic β_2AR +/+; $n = 3$; $ $P < 0.01$ vs. non-ischaemic β_2AR–/–; @ $P < 0.01$ vs. ischaemic β_2AR–/– alone; $n = 3$).

vascular delivery of adenovirus leads to the infections mostly of vascular cells, including endothelium and VSMC, and perivascular fibroblasts and skeletal myocytes as shown by LacZ staining (Figure S1A and B). Administration by this route of Adβ_2AR in β_2AR–/– mice restores βAR density in the hindlimb (Figure 1A). Gross morphology and functional analysis of mice following chronic ischaemia indicate a higher occurrence of necrosis, autoamputation and limping in β_2AR–/– mice as compared to β_2AR+/+ controls (Figure 1B). β_2AR restoration by Adβ_2AR was also able to prevent this symptom (Figure 1B). US evaluation of hindlimb perfusion (blood flow, BF) immediately after femoral artery removal shows an absence of flow in ischaemic HL in all groups of mice (data not shown). Over two weeks, BF was partially restored in β_2AR+/+ while no improvement was observed in β_2AR–/– mice (Figure 1C). A similar result was obtained with the dyed beads perfusion analysis (Figure 1D). As assessed by both techniques, the Adβ_2AR restores blood perfusion through the ischaemic hindlimb (Figure 1C and D). In line with these results, chronic ischaemia appeared to induce a capillary rarefaction that was higher in the β_2AR–/– compared to the β_2AR+/+ mice, and Adβ_2AR reversed this effect in the β_2AR–/– (Figure 1E). β_1AR mRNA levels were not affected by the β_2AR removal, nor by Adβ_2AR gene therapy (Figure S1C). We thus evaluated the production of reactive VEGF in the ischaemic hindlimb. Consistent with the perfusion data, VEGF gene expression was upregulated in the ischaemic hindlimbs of β_2AR+/+ mice, while it was blunted in the β_2AR–/– mice both before and after ischaemia (Figure 1F). In the latter, Adβ_2AR gene therapy restored the VEGF level in basal conditions as well during chronic ischaemia (Figure 1F).

Evaluation of angiogenic phenotypes in vitro

Matrigel assay and VEGF production in primary cultures of ECs. In order to study angiogenesis *in vitro*, we tested the ability of mouse EC primary cultures to organize into a network when plated on a matrigel substrate. β_2AR gene deletion inhibited the ability of ECs to form into vascular tubes compared to wild-type cells (Figure 2A). To verify the relevance of NFκB to the pro-angiogenic phenotype of EC, we transfected β_2AR+/+ cells with the NFκB inhibitor IκB, 48 h before plating cells on matrigel. As expected, IκB blocked the tubular formation of β_2AR+/+ endothelial cells on matrigel (Figure 2B). We further investigated the pro-angiogenic phenotype of β_2AR–/– ECs by evaluating VEGF production in basal conditions and after isoprenaline treatment. As shown in Figures 2C and 6 h of stimulation with Iso increased VEGF levels in β_2AR+/+ but not in β_2AR–/– EC. A similar result was obtained when VEGF mRNA levels were determined by RT-PCR in the same conditions (Figure 2D).

β2AR effects on NFκB signalling. To investigate the ability of β_2ARs to modulate VEGF production and angiogenesis, we tested the possibility that β_2AR may regulate the activity of the NFκB transcription factor. Indeed, in β_2AR+/+ EC, βAR

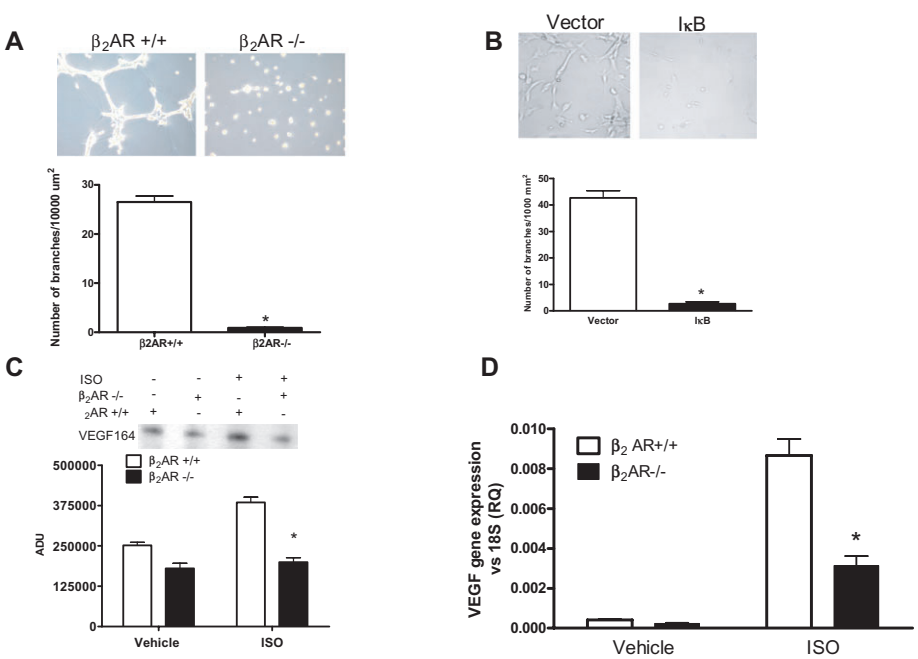

Figure 2

β_2AR gene deletion inhibits VEGF production and vascular tube formation *in vitro*. (A) Vascular tube formation of endothelial cells (ECs) was assessed on matrigel. β_2AR–/– and β_2AR+/+ control ECs (2×10^5) were incubated at 37°C for 12 h in 1 mL DMEM. Representative fields were taken, and the average of the total number of complete tubes was counted in 15 random fields by two independent investigators (*$P < 0.05$ vs. β_2AR+/+ EC, 3 experiments). (B) Vascular tube formation of β_2AR+/+ ECs (2×10^5) transfected with an empty Vector or a plasmid encoding for IkB was assessed on matrigel. Cells were treated as above. (* $P < 0.05$ vs. Vector, 3 experiments). (C) VEGF production in ECs measured by Western blot of extracellular medium. (* $P < 0.05$ vs. β_2AR+/+; $n = 3$ per group). (D) VEGF mRNA in ECs measured by RT-PCR. (* $P < 0.05$ vs. β_2AR+/+; $n = 3$ per group).

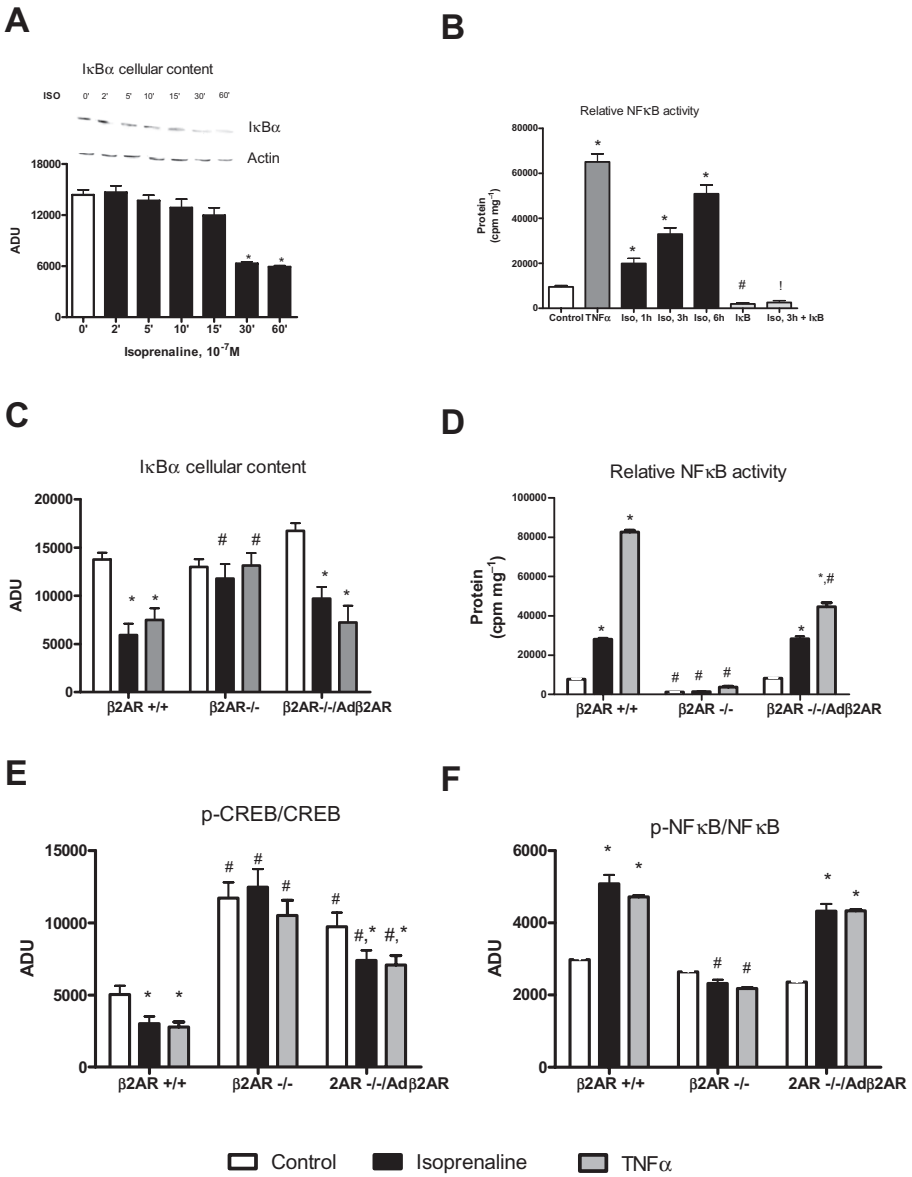

Figure 3

Effects of β_2AR gene deletion on NFκB signalling. (A) IκBα levels visualized by Western blot in β_2AR+/+ ECs. Isoprenaline (Iso, 10^{-7} M) was kept in the tissue culture medium for the time indicated. Densitometry units (ADU) (results normalized to actin response) are depicted in graphs. (* $P <$ 0.05 vs. control, $n = 3$). (B) Effects of TNFα (20 ng·mL^{-1}) for 6 h or Iso (10^{-7} M) for 1, 3 and 6 h on NFκB transcription activity in β_2AR+/+ EC and in β_2AR+/+ EC transfected with the IκB plasmid (* $P < 0.05$ vs. control, # $P < 0.05$ vs. control; ! $P < 0.05$ Iso + IκB vs. IκB; $n = 3$ to 5). (C) IκBα levels assessed by Western blot in β_2AR–/– and β_2AR+/+ ECs stimulated with Iso (10^{-7} M, 1 h) or TNFα (20 ng·mL^{-1}, 1 h) (* $P < 0.05$ vs. control; # $P < 0.05$ vs. β_2AR+/+; $n = 3$ to 5). (D) NFκB activity in EC induced by Iso (10^{-7} M) and TNFα (20 ng·mL^{-1}) (* $P < 0.05$ vs. control; # $P < 0.05$ vs. β_2AR +/+; $n = 3$ to 5). (E) ECs were stimulated with Iso (10^{-7} M) and TNFα (20 ng·mL^{-1}). CREB phosphorylation was visualized by Western blot, digitalized and corrected for endogenous CREB. (* $P < 0.05$ vs. control; # $P < 0.05$ vs. β_2AR +/+, $n = 3$). (F) EC were stimulated as in (E), and NFκB phosphorylation was visualized by WB, digitalized and corrected for total NFκB. (* $P < 0.05$ vs. control; # $P < 0.05$ vs. β_2AR +/+, $n = 3$).

stimulation with Iso induced a time-dependent degradation of the endogenous NFκB inhibitor, IκBα (Figure 3A). Consistent with this result, the luciferase assays demonstrated a time-dependent increase in NFκB transcriptional activity after Iso stimulation (Figure 3B). As expected, TNFα also increased NFκB transcriptional activity in β_2AR+/+ EC, and the overexpression of IκB inhibited the Iso-induced increase in NFκB activity (Figure 3B).

In ECs, β_2AR gene deletion inhibits Iso-induced IκBα downregulation (Figure 3C), confirming that β_2AR may regulate NFκB activation in response to Iso. Surprisingly, β_2AR gene deletion also inhibited TNFα-induced IκBα downregulation (Figure 3C). Accordingly, restoration of β_2ARs by means of Adβ_2AR infection corrected both Iso and TNFα–mediated IκBα degradation to levels comparable to the ones observed in β_2AR+/+ EC (Figure 3C), confirming the importance of

β_2ARs in NFκB endothelial signalling. In accord with this, in β_2AR–/– EC, both Iso and TNFα-induced NFκB-activity were blocked, and Adβ_2AR restored the responses to both agonists (Figure 3D). These data suggest that β_2AR knock-out may have a general impact on cytokine transcription.

Recently, CREB, another β_2AR-controlled transcription factor, has been shown to down-regulate the activity of NFκB (Ye, 2001). Indeed, CREB binding protein (CBP) and the related cofactor p300 are co-activators able to regulate the activity of transcription factors, and CREB and NFκB have been shown to compete for limiting amounts of CBP/p300 (Ye, 2001). In fact, the recruitment of these co-activators by CREB reduces their availability for NFκB. Thus, we evaluated CREB and NFκB activation by Western blot in β_2AR–/– ECs stimulated with Iso or TNFα. β_2AR gene deletion increased CREB phosphorylation both in basal conditions and after stimulation with Iso or TNFα and the restoration of β_2ARs by adenovirus-mediated gene transfer decreased p-CREB levels (Figure 3E). Reciprocal results were obtained with NFκB. Indeed, compared to β_2AR proficient controls, in β_2AR–/– ECs, Iso and TNFα failed to induce NFκB phosphorylation while Adβ_2AR infection restored the responses to both agonists (Figure 3F).

Identification of signal transduction components. To determine whether CREB upregulation is a common mechanism of inhibition for β_2AR and TNFR stimulation of NFκB, we assessed pNFκB after stimulation with Iso or TNFα in β_2AR+/+ EC trasfected with CREB or IkB. Indeed, both substances resulted in the inhibition of NFκB activation to both agonists (Figure 4A). Given the ability of the β_2AR to couple to both Gs and Gi, we tested the possibility that Gi is indeed involved in

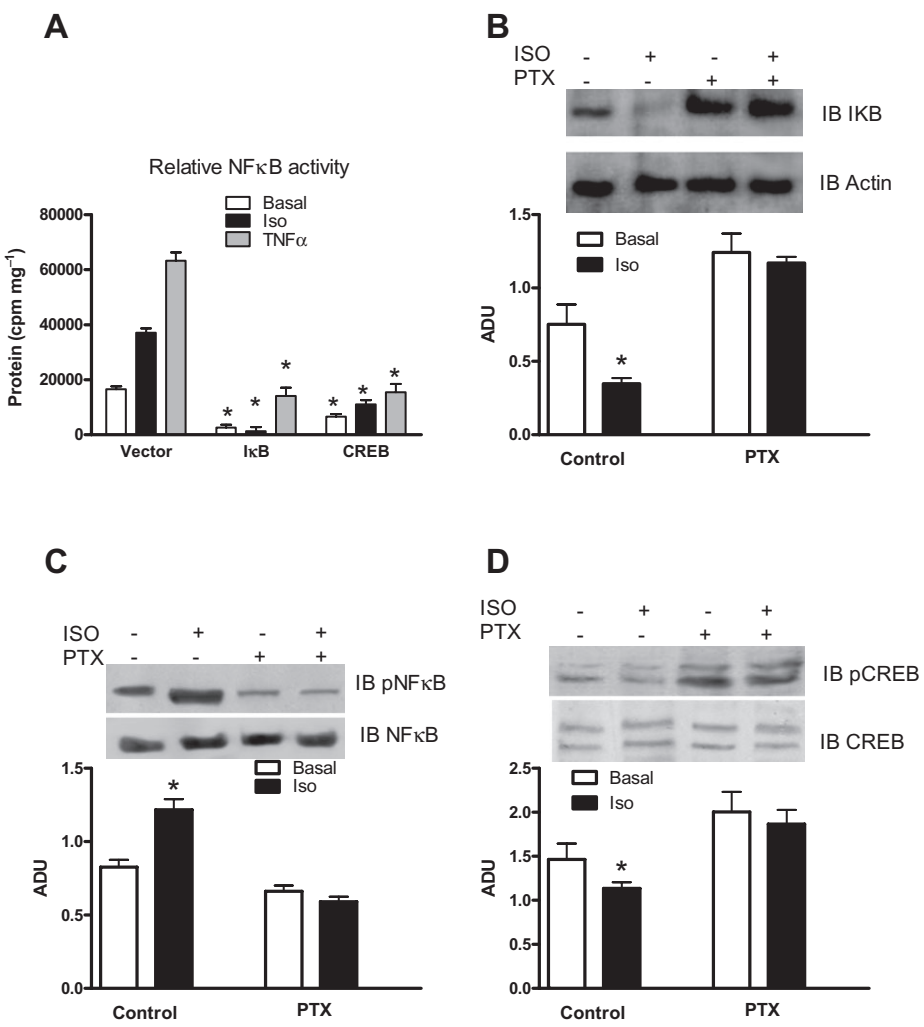

Figure 4

Molecular mechanisms involved in β_2AR activation of NFκB. (A) Effects of transgenic expression of IκB and CREB in β_2AR +/+ EC on NFκB activation in response to Iso (10^{-7} M, 3 h) and TNFα (20 ng·mL^{-1}). *P < 0.05 vs. Vector, n = 3. (B) Evaluation by Western blot of β_2AR +/+ EC of the effects of pertussis toxin (PTX, 10^{-4} M) on Iso-induced IκB downregulation. * P < 0.05 vs. basal, n = 4; ADU: arbitrary densitometric units. (C) Evaluation by Western blot of β_2AR+/+ EC of the effects of pertussis toxin (PTX, 10^{-4} M) on Iso-induced NFκB phosphorylation. *P < 0.05 vs. basal, n = 4. (D) Evaluation by Western blot of β_2AR+/+ EC of the effects of pertussis toxin (PTX, 10^{-4} M) on Iso-induced CREB dephosphorylation. * P < 0.05 vs. basal, n = 4.

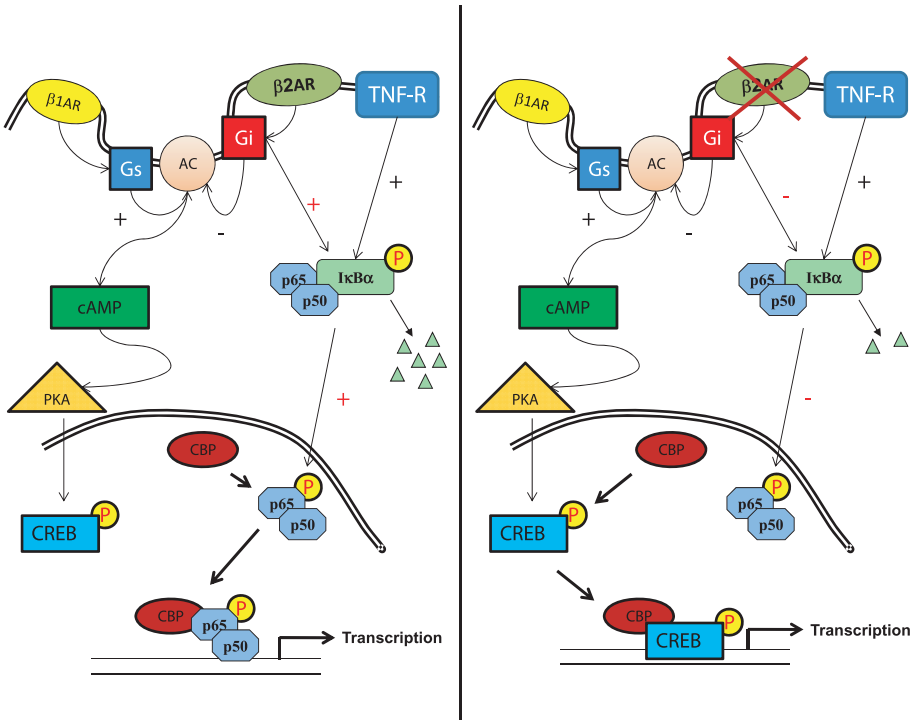

Figure 5

In the wild-type cell (left), the presence of the β_2AR causes a tonic stimulation that fosters the activation of NFκB, which, by translocating to the nucleus upon activation, competes for CBP with CREB. Furthermore, the β_2AR exerts a tonic inhibition on cAMP production, by coupling to Gi. Once the receptor is removed (right), the inhibitory effect on cAMP is released, unbalancing the nuclear transcription towards CREB, which binds more CBP, thus making NFκB binding to the same cofactor unlikely to occur. pP65/p50: NFκB; TNFR: TNFα receptor.

maintaining low levels of CREB within the cell. To test this hypothesis, we treated cells with the Gi inhibitor *Pertussis* toxin for 18 h and then stimulated β_2AR+/+ ECs with Iso. Gi inhibition was accompanied by the inhibition of Iso-induced IκB downregulation (Figure 4B) and NFκB phosphorylation (Figure 4C). Furthermore, PTX increased the basal level of pCREB and prevented Iso-induced dephosphorylation of CREB (Figure 4D).

Finally, we have presented these new findings in a cartoon as shown in Figure 5.

Discussion

The results of our study provide compelling evidence that the removal of the β_2AR impairs angiogenesis both *in vitro* and *in vivo*. This finding extends previous knowledge regarding the ability of β_2AR overexpression to enhance angiogenesis *in vivo*, and it further supports the knowledge of the ability of β_2AR to induce VEGF and cytokine production. Indeed, our work adds novel findings concerning the signalling that connects β_2ARs and the nuclear transcriptional activity of NFκB.

Evidence has been obtained suggesting that the adrenergic system is activated within ischaemic regions (Newton *et al.*, 1997) but the physiological relevance of this response is unclear. A teleological explanation would suggest that this activation is needed to better adapt to the ischaemic stress. Indeed, the regenerative properties of catecholamines have been implicated by the observation that catecholamine-deficient mice undergo inappropriate embryo development (Zhou *et al.*, 1995). During postnatal life, catecholamines participate in cardiac and vascular remodelling and in tissue regeneration in response to various stresses (Iaccarino *et al.*, 2001a; Ciccarelli *et al.*, 2008). Adrenoceptors are the effectors of catecholamines, but their role appears to be redundant, since correct embryo development occurs in all of the AR knock-out models, and in adult life, mice with deletion of AR genes do not present basal phenotypic alterations. Under stress conditions, though, or in the presence of catecholamine challenge, a perturbation in the phenotype of KO mice has been noted (Rohrer *et al.*, 1999). In particular, previous studies in βAR–/– mice have shown that β_2ARs are mostly involved in vascular and metabolic mechanisms (Chruscinski *et al.*, 1999; Rohrer *et al.*, 1999). Our study extends this notion and is the first to illustrate the requirement for endogenous β_2ARs in neoangiogenesis following chronic ischaemia, by providing the following evidence: (i) β_2AR–/– mice present impaired tolerance to chronic ischaemia; (ii) this phenotype is rescued by the local restoration of β_2AR membrane-density, induced by adenoviral-mediated gene transfer; (iii) a functional relationship appears to exist between the β_2AR and NFκB, the transcription factor involved in ischaemia-induced cytokine production.

These results accord with our recent observation that overexpression of the β_2AR enhances the adaptive pro-

angiogenic response to ischaemia (Iaccarino *et al.*, 2005). Importantly, the present results add to the hypothesis that other endogenously expressed βAR subtypes cannot undertake this role of β_2ARs in ischaemic neo-angiogenesis. Intimate differences in the signalling capabilities of this receptor make it unique, and probably this is the reason for our findings. Removal of this receptor alters the intracellular signal transduction pathways to such an extent that the trascriptional status of the cell is modified. Our *in vitro* study revealed that angiogenesis is impaired in β_2AR–/– EC, probably due to the impaired production of cytokines such as VEGF. The main transcription factors modulating VEGF expression are hypoxia-inducible factor-1α (HIF-1α) (Marti *et al.*, 2000) and NFκB (Kiriakidis *et al.*, 2003). HIF-1α activates the transcription of target genes in response to hypoxia and is inactive in basal conditions due to ubiquitination and degradation. NFκB, in contrast, can be activated following stimulation of different receptors. The ability of GPCRs to activate this transcription factor has been established in different cell types, mainly in the immune system. With regard to the βARs, the evidence showing that βAR agonists are able to induce NFκB activation is controversial. In monocytes, Farmer and Pugin (2000) showed that a number of βAR agonists had inhibitory effects on LPS-induced TNFα and IL-8 production, and proposed that cAMP through PKA is the mediator of such inhibition (Farmer and Pugin, 2000). In contrast, Chandrasekar *et al.* (2004) showed that in cardiac-derived ECs, Iso induces NFκB promoter activity in a β_2AR-dependent manner. These authors concluded that β_2ARs induce NFκB activation in a cAMP-independent manner, through the activation of Gi, Pi3K, Akt and IKK with IκBα degradation. Our results accord with the latter findings, since in β_2AR+/+ EC, Iso induced IκBα degradation and enhanced NFκB transcriptional activity in a time-dependent manner. Furthermore, our data indicate that the physical presence of β_2ARs is needed to activate NFκB; indeed, β_2AR gene deletion inhibited NFκB activity in response to both GPCRs and TNF-Rs. Gαs and Gαi signalling pathways have opposite effects on NFκB: Gs-dependent signalling, induces PKA-dependent CREB activation and consequently inhibition of NFκB activity (Ye, 2001). In contrast, Gi activates NFκB by inhibiting/removing IκB. Our hypothesis is that the lack of β2ARs that have the ability to couple to Gi tilts the balance towards Gs-dependent signalling, which would lead to PKA-induced CREB activation and CBP/p300 recruitment, making the latter unavailable for NFκB activation (Figure 5). Indeed, validation of such a hypothesis derives from our studies with the pertussis toxin, showing the relevance of Gi for β_2AR-induced activation of NFκB. Irrespective of this result, the observation that regardless of its mechanism of action β_2AR influenced not only isoprenaline, but also TNFα-dependent activation of NFκB is strongly suggestive of a pivotal role played by β_2ARs in the instruction of signals required for the fine-tuning of NFκB transcriptional activity. We have performed our experiments in the endothelial cells, but it is most likely that the β_2AR can regulate NFκB activity also in other cell types. In particular it would be interesting to evaluate the skeletal muscle, which expresses a large number of β_2ARs and is also an important source of VEGF.

In conclusion, our data indicate that the β_2AR is important in mediating production of key pro-angiogenic cytokines, such as VEGF. The impairment of the signal transduction of this receptor results in imparment of angiogenesis in response to chronic ischaemia. Our data add a novel piece to the puzzling paradigm of those pathophysiological conditions that are characterized by increased adrenergic neural drive, impaired β adrenoceptor signalling and impaired organ function such as myocardial ischaemia. Under these conditions, the reduction of β_2ARs signalling is detrimental not only for the cardiac function but also for the development of an adequate compensatory neoangiogenesis, which would worsen the blood supply to the ischaemic heart and accelerate the progression of myocardial dysfunction. The use of therapeutic strategies aimed at improving βAR signalling, may therefore achieve double efficacy, by ameliorating myocardial function and by hastening compensatory angiogenesis.

Acknowledgements

Fundings to GI from Italian Ministry of Research, PRIN 20074MSWYW.

Conflict of interest

The authors declare that they have no competing financial interests.

References

Alexander SPH, Mathie A, Peters JA (2009). Guide to Receptors and Channels (GRAC), 4th Edition. Br J Pharmacol 158 (Suppl. 1): S1–254.

Chandrasekar B, Marelli-Berg FM, Tone M, Bysani S, Prabhu SD, Murray DR (2004). Beta-adrenergic stimulation induces interleukin-18 expression via beta2-AR, PI3K, Akt, IKK, and NF-kappaB. Biochem Biophys Res Commun 319: 304–311.

Chruscinski AJ, Rohrer DK, Schauble E, Desai KH, Bernstein D, Kobilka BK (1999). Targeted disruption of the beta2 adrenergic receptor gene. J Biol Chem 274: 16694–16700.

Ciccarelli M, Cipolletta E, Santulli G, Campanile A, Pumiglia K, Cervero P *et al.* (2007). Endothelial beta2 adrenergic signaling to AKT: role of Gi and SRC. Cell Signal 19: 1949–1955.

Ciccarelli M, Santulli G, Campanile A, Galasso G, Cervero P, Altobelli GG *et al.* (2008). Endothelial alpha1-adrenoceptors regulate neo-angiogenesis. Br J Pharmacol 153: 936–946.

Farmer P, Pugin J (2000). Beta-adrenergic agonists exert their 'anti-inflammatory' effects in monocytic cells through the IkappaB/NF-kappaB pathway. Am J Physiol Lung Cell Mol Physiol 279: L675–L682.

Ferro A, Queen LR, Priest RM, Xu B, Ritter JM, Poston L *et al.* (1999). Activation of nitric oxide synthase by beta 2-adrenoceptors in human umbilical vein endothelium in vitro. Br J Pharmacol 126: 1872–1880.

Iaccarino G, Tomhave ED, Lefkowitz RJ, Koch WJ (1998). Reciprocal in vivo regulation of myocardial G protein-coupled receptor kinase expression by beta-adrenergic receptor stimulation and blockade. Circulation 98: 1783–1789.

Iaccarino G, Barbato E, Cipoletta E, Fiorillo A, Trimarco B (2001a). Role of the sympathetic nervous system in cardiac remodeling in hypertension. Clin Exp Hypertens 23: 35–43.

Iaccarino G, Barbato E, Cipolleta E, Esposito A, Fiorillo A, Koch WJ *et al*. (2001b). Cardiac betaARK1 upregulation induced by chronic salt deprivation in rats. Hypertension 38: 255–260.

Iaccarino G, Cipolletta E, Fiorillo A, Annecchiarico M, Ciccarelli M, Cimini V *et al*. (2002). Beta(2)-adrenergic receptor gene delivery to the endothelium corrects impaired adrenergic vasorelaxation in hypertension. Circulation 106: 349–355.

Iaccarino G, Ciccarelli M, Sorriento D, Cipolletta E, Cerullo V, Iovino GL *et al*. (2004). AKT participates in endothelial dysfunction in hypertension. Circulation 109: 2587–2593.

Iaccarino G, Ciccarelli M, Sorriento D, Galasso G, Campanile A, Santulli G *et al*. (2005). Ischemic neoangiogenesis enhanced by beta2-adrenergic receptor overexpression: a novel role for the endothelial adrenergic system. Circ Res 97: 1182–1189.

Kiriakidis S, Andreakos E, Monaco C, Foxwell B, Feldmann M, Paleolog E (2003). VEGF expression in human macrophages is NF-kappaB-dependent: studies using adenoviruses expressing the endogenous NF-kappaB inhibitor IkappaBalpha and a kinase-defective form of the IkappaB kinase 2. J Cell Sci 116: 665–674.

Lembo G, Iaccarino G, Vecchione C, Barbato E, Izzo R, Fontana D *et al*. (1997). Insulin modulation of an endothelial nitric oxide component present in the alpha2- and beta-adrenergic responses in human forearm. J Clin Invest 100: 2007–2014.

Marti HJ, Bernaudin M, Bellail A, Schoch H, Euler M, Petit E *et al*. (2000). Hypoxia-induced vascular endothelial growth factor expression precedes neovascularization after cerebral ischemia. Am J Pathol 156: 965–976.

Newton GE, Adelman AG, Lima VC, Seidelin PH, Schampaert E, Parker JD (1997). Cardiac sympathetic activity in response to acute myocardial ischemia. Am J Physiol 272: H2079–2084.

Rohrer DK, Chruscinski A, Schauble EH, Bernstein D, Kobilka BK (1999). Cardiovascular and metabolic alterations in mice lacking both beta1- and beta2-adrenergic receptors. J Biol Chem 274: 16701–16708.

Santulli G, Ciccarelli M, Palumbo G, Campanile A, Galasso G, Ziaco B *et al*. (2009a). In vivo properties of the proangiogenic peptide QK. J Transl Med 7: 41.

Santulli G, Cipolletta E, Campanile A, Maione S, Trimarco V, Marino M *et al*. (2009b). Deletion of the CaMK4 Gene in Mice Determines a Hypertensive Phenotype. Circulation 120: S613–S613.

Shenoy SK, Drake MT, Nelson CD, Houtz DA, Xiao K, Madabushi S *et al*. (2006). beta-arrestin-dependent, G protein-independent ERK1/2 activation by the beta2 adrenergic receptor. J Biol Chem 281: 1261–1273.

Sorriento D, Campanile A, Santulli G, Leggiero E, Pastore L, Trimarco B *et al*. (2009). A new synthetic protein, TAT-RH, inhibits tumor growth through the regulation of NFkappaB activity. Mol Cancer 8: 97.

Sorriento D, Santulli G, Fusco A, Anastasio A, Trimarco B, Iaccarino G (2010). Intracardiac injection of AdGRK5-NT reduces left ventricular hypertrophy by inhibiting NF-{kappa}B-Dependent hypertrophic gene expression. Hypertension 56: 696–704.

Ye RD (2001). Regulation of nuclear factor kappaB activation by G-protein-coupled receptors. J Leukoc Biol 70: 839–848.

Zhou QY, Quaife CJ, Palmiter RD (1995). Targeted disruption of the tyrosine hydroxylase gene reveals that catecholamines are required for mouse fetal development. Nature 374: 640–643.

Zhou RH, Lee TS, Tsou TC, Rannou F, Li YS, Chien S *et al*. (2003). Stent implantation activates Akt in the vessel wall: role of mechanical stretch in vascular smooth muscle cells. Arterioscler Thromb Vasc Biol 23: 2015–2020.

Supporting information

Additional Supporting Information may be found in the online version of this article:

Figure S1 Efficient gene delivery via femoral artery catheterization (A-B). Recombinant LacZ Adenovirus was delivered to the ischemic hindlimb via catheterization as described in the Methods section and results in gene transduction of capillaries (A) as well as perivascular muscle fibers (B). Muscle β1AR mRNA levels measured by RT-PCR (C). Hindlimb muscles processed as described in methods showing unmodified β1AR mRNA levels among β2AR +/+, β2AR–/– and Adβ2AR treated mice.

Please note: Wiley-Blackwell are not responsible for the content or functionality of any supporting materials supplied by the authors. Any queries (other than missing material) should be directed to the corresponding author for the article.